PHYSICAL REVIEW B **74**, 094427 (2006)

Tuning the electrical properties of $La_{0.75}Ca_{0.25}MnO_3$ thin films by ferroelectric polarization, ferroelectric-field effect, and converse piezoelectric effect

R. K. Zheng,[1,*] Y. Wang,[1] J. Wang,[1] K. S. Wong,[1] H. L. W. Chan,[1] C. L. Choy,[1] and H. S. Luo[2]
[1]*Department of Applied Physics and Materials Research Center, The Hong Kong Polytechnic University, Hong Kong, China*
[2]*State Key Laboratory of High Performance Ceramics and Superfine Microstructure, Shanghai Institute of Ceramics, Chinese Academy of Sciences, Shanghai 201800, China*

(Received 4 December 2005; revised manuscript received 23 July 2006; published 26 September 2006)

Thin films of $La_{0.75}Ca_{0.25}MnO_3$ (LCMO) have been grown on ferroelectric $(1-x)Pb(Mg_{1/3}Nb_{2/3})O_3$-$xPbTiO_3$ ($x\sim0.33$) single-crystal substrates. The ferroelectric polarization in the PMN-PT substrates gives rise to a decrease in resistance and an upward shift in Curie temperature of the LCMO films, which was interpreted in terms of the ferroelectric polarization induced lattice strain effect. The resistance of the LCMO films can be modulated by applying dc/ac electric fields across the polarized PMN-PT substrates. The electric field induces lattice strains in the PMN-PT substrates via the converse piezoelectric effect, which subsequently changes the strain state and resistance of the LCMO films. A quantitative relation between the resistance in the LCMO films and the induced lattice strains in the PMN-PT substrates has been established. Moreover, we identified that the ferroelectric polarization and converse piezoelectric effect induced lattice strain effects dominate over the field effect in the LCMO/PMN-PT systems.

DOI: 10.1103/PhysRevB.74.094427 PACS number(s): 77.84.−s, 75.47.Lx, 73.50.−h, 77.65.−j

I. INTRODUCTION

The perovskite-type $R_{1-x}A_xMnO_3$ (R and A are trivalent rare-earth and divalent alkaline-earth ions, respectively) manganites have received a great deal of interest in recent years because of a variety of interesting properties such as colossal magnetoresistance (CMR) and charge, spin, and orbital orderings.[1] Stimulated by the potential applications of CMR materials, a considerable amount of earlier work has focused on growing thin films in order to achieve a large low-field CMR effect. Accumulated theoretical and experimental studies have shown that the lattice strain due to the lattice mismatch between substrates and thin films plays a very important role in determining the properties of thin films, e.g., Curie temperature, resistivity, magnetic anisotropy, magnitude of CMR, and electronic phase separation.[2–10] The lattice strain effect has been interpreted qualitatively within the double-exchange model in which the hopping matrix element t could be modified by lattice strain through changing Mn-O bond length and/or Mn-O-Mn bond angle. Compressive strain usually reduces resistivity and shifts Curie temperature T_C upward while tensile strain gives rise to opposite effects on resistivity and T_C. However, recent studies showed that compressive strain does not always lead to enhancement of T_C. In contrast, tensile strain enhances T_C.[10–13] Moreover, it is believed that compressive (tensile) strain could lead to a decrease (increase) in the Mn-O bond length. The experimental measurements in $La_{0.67}Sr_{0.33}MnO_3$ (Ref. 14) and $La_{1-x}Ca_xMnO_3$ ($x=0.31,0.39$) (Ref. 15) thin films, however, showed that Mn-O bond lengths remain the same as that of bulk materials, no matter whether the thin films are under compressive or tensile strain. In addition, a mechanism involving the orbital degree of freedom has also been proposed to explain the anomalous lattice strain effect in $La_{1-x}Ba_xMnO_3$ thin films.[10,16] All these features demonstrate that the detailed effects of lattice strain on electrical and magnetic properties of manganite thin films are far from being fully understood and would require further investigation and discussion.

Strained thin films are usually obtained by growing thin films of various thickness on substrates with different lattice parameters.[8–14] However, other negative variables, e.g., oxygen nonstoichiometry, crystalline quality, lattice relaxation, grain size, and variation in chemical composition, also have a significant impact on the properties of thin films.[17–19] Therefore, it becomes relatively difficult to isolate property changes due to lattice strain effect from those resulting from these negative variables. In this regard, it would be of value to examine the effects of lattice strain on thin-film properties with the *same* thin-film sample in which the strain state of thin films could be *in situ* varied while the negative variables could be kept fixed. A realization of such control over the strain state of thin films would help one gain further insight into the substrate-induced lattice strain effect.

The relaxor-based $(1-x)Pb(Mg_{1/3}Nb_{2/3})O_3$-$xPbTiO_3$ (PMN−xPT) single crystals with compositions near the morphotropic phase boundary are ferroelectric materials that exhibit outstanding piezoelectric activity.[20,21] PMN−xPT single crystals have perovskite structure and are lattice-matched to $R_{1-x}A_xMnO_3$ manganites, which makes them good substrates for the growth of manganite thin films. Moreover, the PMN−xPT have large remnant ferroelectric polarization and low coercive field and may be good materials for use as gate insulators in manganite-based ferroelectric-field effect transistors. Furthermore, if ferroelectric PMN−xPT is used as a substrate, the lattice strain in PMN−xPT substrate and the subsequent strain state of thin films grown on it can be controlled by ferroelectric polarization and converse piezoelectric effect of PMN−xPT.

In this paper, we report the electrical properties of $La_{0.75}Ca_{0.25}MnO_3$ (LCMO) thin films grown on ferroelectric PMN-PT single-crystal substrates. We tuned the strain state and resistance of the LCMO films by ferroelectric polarization and the converse piezoelectric effect of PMN-PT. These

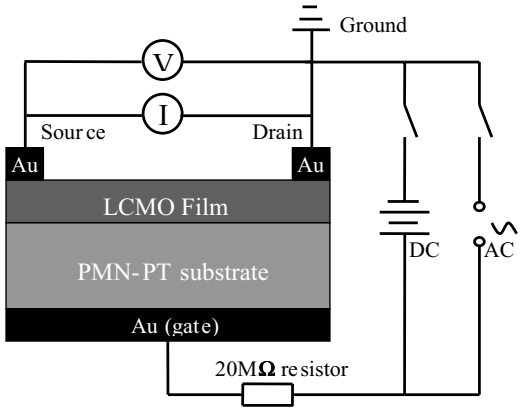

FIG. 1. Schematic diagram showing the LCMO/PMN-PT structure in FET configuration and the circuit for electrical measurements.

approaches for changing the strain state of thin films via ferroelectric polarization and converse piezoelectric effect provide new routes to tune the properties of manganite thin films.

II. EXPERIMENTAL PROCEDURES

PMN-PT single crystals of dimensions Φ40 mm $\times$80 mm were grown by a modified Bridgman technique at the Shanghai Institute of Ceramics. The experimental details for the growth of the PMN-PT single crystals have been described elsewhere.[22] The single crystals were cut into plates of dimensions 10 mm$\times$3.5 mm$\times$0.4–0.5 mm and with the plate normal in the ⟨001⟩ crystal direction, and polished until the average surface roughness was less than 1 nm. The LCMO films were deposited on the (001)-oriented PMN-PT substrates by dc magnetron sputtering in an argon-oxygen flow at a pressure of 4.35 Pa and at a substrate temperature of 680 °C. After deposition, the LCMO films were slowly cooled to room temperature *in situ* and postannealed in air at 700 °C for 30 min.

Resistance of the LCMO films was examined in the ferroelectric–field-effect-transistor (FET) configuration as shown in Fig. 1. Electric voltages were applied to the PMN-PT layer through the gate and the drain. A resistor of 20 MΩ was connected in series with the gate in order to protect the current source and voltage meters in case a dielectric breakdown took place in the PMN-PT layer.

X-ray diffraction (XRD) measurements were made using a Bruker D8 Discover x-ray diffractometer equipped with Cu $K\alpha$ radiation. Thickness of the LCMO films was examined using a field-emission scanning electron microscope (JEOL JSM-6335F). A room-temperature ferroelectric hysteresis loop of the PMN-PT substrate was measured using a standard Sawyer-Tower circuit at 10 Hz. The strain hysteresis loop of the PMN-PT substrate caused by the converse piezoelectric effect was measured by a piezoresponse force microscopy using a scanning probe microscope (Nanoscope IV, Digital Instruments) equipped with a conductive tip coated with Pt.

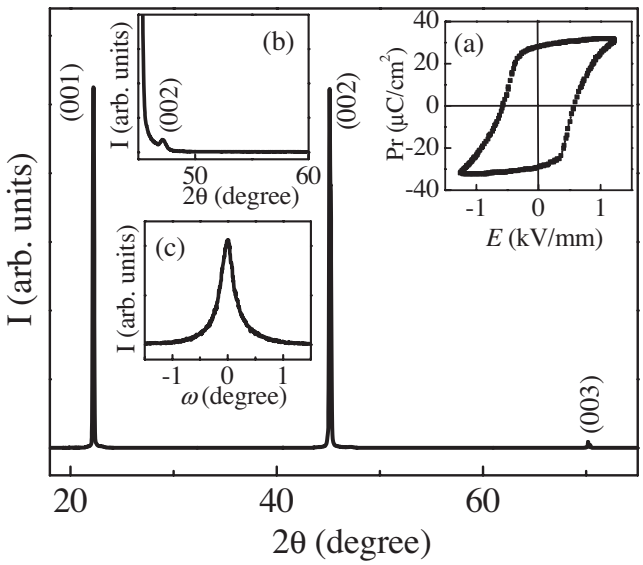

FIG. 2. A typical θ-2θ XRD pattern of LCMO/PMN-PT structure. Inset (a) shows the room-temperature ferroelectric hysteresis loop of the PMN-PT substrate. Inset (b) shows the expanded view of the θ-2θ XRD pattern of the PMN-PT and LCMO (002) reflections. Inset (c) shows the rocking curve of the LCMO (002) reflection.

III. RESULTS AND DISCUSSION

Figure 2 shows a typical θ-2θ XRD pattern of the LCMO/PMN-PT structure. There appear strong (00l) (l=1,2,3) reflections resulting from the PMN-PT substrate. This, together with the square ferroelectric hysteresis loop [inset (a) of Fig. 2], indicates that the PMN-PT substrate is of good quality. It is noted that the reflections from the LCMO film have been covered up by the strong reflections from the PMN-PT substrate. The inset (b) of Fig. 2 shows the expanded view of the PMN-PT and LCMO (002) reflections for the LCMO/PMN-PT structure. It can be seen that there appears a weak LCMO(002) reflection on the right-hand side of the PMN-PT(002) reflection, indicating that the LCMO film grows preferentially c-axis oriented. The rocking curve taken around the LCMO(002) reflection has a full width at half maximum of ~0.29°, as shown in the inset (c) of Fig. 2.

Figure 3(a) shows the temperature dependence of the resistance for the LCMO film with a thickness of ~25 nm when the PMN-PT substrate is in different polarization states. When the PMN-PT is in an unpolarized state (referred to as P_r^0), the resistance of the LCMO film increases with decreasing temperature from 335 K to a lower temperature and reaches a maximum near the insulator to metal transition temperature T_P. With further decrease in temperature, the LCMO goes into a ferromagnetic state and the resistance decreases rapidly. To examine the effects of ferroelectric polarization and the ferroelectric-field effect on the resistance of the LCMO film, we applied a positive poling voltage of +500 V (corresponding to an electric field of E ~ +1.2 kV/mm, much larger than the coercive field of the PMN-PT) to the gate so that the PMN-PT substrate was positively polarized (referred to as P_r^+). The resistance of the

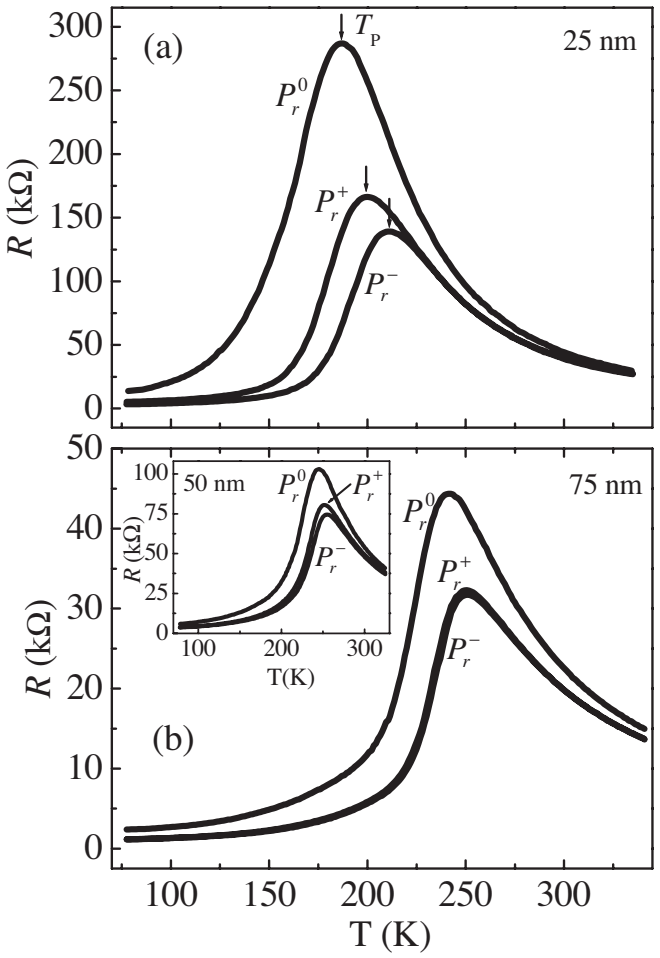

FIG. 3. Temperature dependence of the resistance for the LCMO films when the PMN-PT substrate is in different polarization states. P_r^0, P_r^+, and P_r^- represent unpolarized, positively polarized, and negatively polarized states, respectively.

LCMO film between the source and the drain was measured after the +1.2 kV/mm poling electric field was turned off. As seen in Fig. 3(a), the resistance of the LCMO film decreases over a wide temperature range after the PMN-PT substrate has been positively polarized. The decrease in the resistance is particularly pronounced near T_P where the resistance decreases by ~83%. Moreover, T_P shifts upward by ~13 K.

It is known that the LCMO is a *p*-type material; the majority of the charge carriers in the LCMO film are holes. The application of a positive (or negative) voltage to the gate will polarize the PMN-PT layer such that the electric dipole moments in the PMN-PT point upward (or downward) into the LCMO film, thereby leading to a depletion (or accumulation) of holes in the LCMO film.[23] Thus, if only the ferroelectric-field effect is considered, the resistance of the LCMO film should increase when the PMN-PT layer is positively polarized. Indeed, the resistance of the manganite films in similar manganite-based ferroelectric FET, e.g., $La_{1-x}Ca_xMnO_3$ $(x=0.2,0.3)/Pb(Zr_{0.2}Ti_{0.8})O_3$, $La_{1-x}Ba_xMnO_3(x=0.1,0.15)/Pb(Zr_{0.2}Ti_{0.8})O_3$, $La_{0.8}Sr_{0.2}MnO_3/Pb(Zr_xTi_{1-x})O_3$, increases when the $Pb(Zr_xTi_{1-x})O_3$ layer is positively polarized.[23–27] It is clear that the ferroelectric-field effect cannot account for the decrease in the resistance in the LCMO film for P_r^+. To clarify this problem, we measured the resistance of the LCMO film as a function of temperature when the PMN-PT layer is in a negatively polarized state (referred to as P_r^-). Once again, the resistance of the LCMO film for P_r^- was measured after the poling electric field was turned off. As presented in Fig. 3(a), the resistance for P_r^- also decreases over a wide temperature range and T_P shifts upward by ~24 K after the PMN-PT has been negatively polarized.

It should be noted that the ferroelectric polarization in the PMN-PT layer not only results in a depletion or accumulation of holes in the LCMO film, but also an expansion of the lattice of the PMN-PT layer along the direction of the electric field. If the latter is considered, the decrease in resistance induced by the ferroelectric polarization and the upward shift of T_P in the LCMO film can be understood on the basis of lattice strain effect. After the PMN-PT has been polarized along the ⟨001⟩ direction, the lattice parameter *c* of the PMN-PT increases because the electric field causes the rotation of polarization in the ferroelectric domains toward the field direction. It has been found that the PMN-PT(002) reflection shifts to a lower 2θ angle after the PMN-PT has been positively polarized. This implies that the ferroelectric polarization has resulted in an increase of the lattice parameter *c* of the PMN-PT. Such a change in the lattice parameter *c* will cause decreases in the in-plane lattice parameters *a* and *b* as a result of the Poisson effect,[28] which can subsequently impose in-plane compressive strains on the LCMO film and thus a decrease of the Jahn-Teller electron-lattice interaction in the LCMO film, thereby favoring delocalizing of the charge carriers.[4–6] Meanwhile, the substrate-imposed compressive strain can also give rise to a decrease in the in-plane Mn-O bond length in the film and thus an enhancement of the double-exchange interaction, which leads to an increase in the hopping of charge carriers. This also results in a decrease in the resistance of the LCMO film.

Although the decrease in the resistance for P_r^+ and P_r^- can be qualitatively understood, it is noted that the magnitudes of the decrease in resistance and increase in T_P for P_r^- are much larger than that for P_r^+, as seen in Fig. 3(a). We have plotted the resistance difference (ΔR) between P_r^+ and P_r^- [$\Delta R = R(P_r^+) - R(P_r^-)$] as a function of temperature in Fig. 4. It can be seen that ΔR reaches the maximum near T_P. As discussed above, the positive polarization of the PMN-PT layer will lead to a depletion of holes in the LCMO film and thus an increase in resistance in the LCMO film while a negative polarization of the PMN-PT layer will cause an accumulation of holes in the LCMO film and thus a decrease in resistance. The former can partially cancel out the decrease in the resistance due to the ferroelectric polarization induced lattice strain effect while the latter gives rise to a further decrease in the resistance in the LCMO film, i.e., ΔR may be caused by the ferroelectric-field effect.

It is known that the ferroelectric-field effect is closely related to the total number of charge carriers in the channel material. For a fixed doping level, the number of charge carriers is usually determined by the thickness of a thin film. If the film is so thin that the number of charge carriers in the film is small, the ferroelectric polarization will lead to a large percentage change in the number of charge carriers and thus

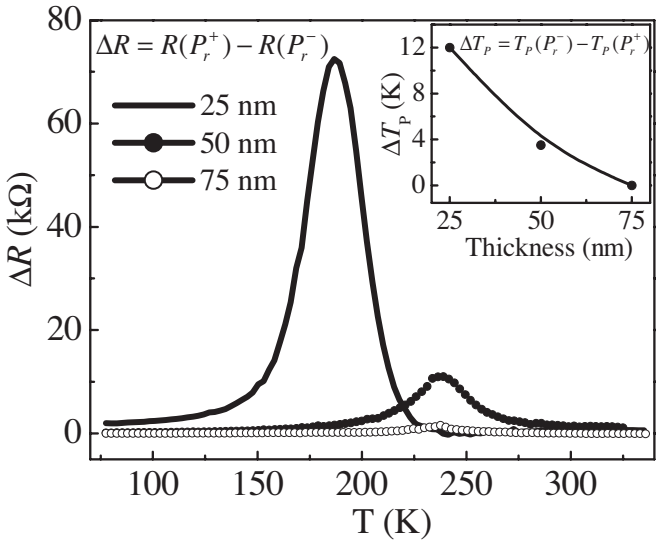

FIG. 4. Temperature dependence of the resistance difference (ΔR) for the LCMO films. Inset shows the thickness dependence of ΔT_P.

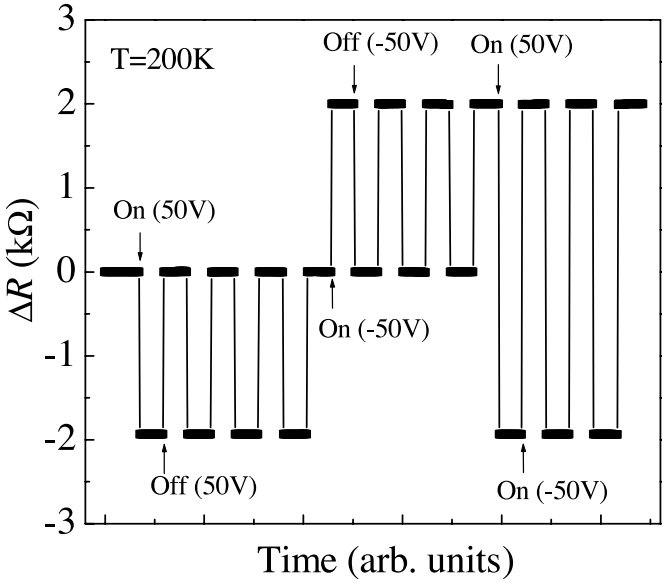

FIG. 5. Resistance response of the LCMO film as a function of time while ±0.12 kV/mm electric fields were switched on and off. Note that the electric fields were applied to the positively polarized PMN-PT substrate.

a strong ferroelectric-field effect.[29] Therefore, for our LCMO/PMN-PT systems with a fixed doping level, the impact of the ferroelectric-field effect on the resistance is expected to be closely related to the thickness of the LCMO films.

To gain insight into the ferroelectric-field effect in the LCMO/PMN-PT structure, we prepared another two LCMO/PMN-PT samples in which the thicknesses of the LCMO films are ~50 and ~75 nm, respectively. We also measured their temperature dependence of resistance when the PMN-PT layer is in different polarization states. As shown in Fig. 3(b), the resistance of the LCMO film with a thickness of ~75 nm decreases over a wide temperature range after the PMN-PT layer has been positively or negatively polarized. However, it should be noted that the resistance and T_P are approximately the same when the PMN-PT layer is in the P_r^+ or P_r^- state. If the ferroelectric-field effect plays a role in influencing the resistance in this sample, the resistance change should show opposite signs when the PMN-PT layer is in the P_r^+ or P_r^- state because of the depletion or accumulation of holes in the LCMO film. Therefore, it can be concluded that the ferroelectric-field effect in this sample is rather limited and the decrease in the resistance for P_r^+ and P_r^- is mainly due to the lattice strain effect as discussed above. For the LCMO film with intermediate thickness (i.e., ~50 nm), the resistance for P_r^- is slightly smaller than that for P_r^+, and T_P for P_r^- is about 3.5 K higher than that for P_r^+, as seen in the inset of Fig. 3(b). It is clear that ΔR and ΔT_P $[\Delta T_P = T_P(P_r^-) - T_P(P_r^+)]$ decrease with increasing thickness of the LCMO films (Fig. 4). Moreover, we note that ΔR reaches the maximum near T_P for all samples but decreases with temperature away from T_P. This feature of ΔR is similar to that observed in manganite-based $La_{1-x}A_xMnO_3(A = Ca, Sr, Ba)/Pb(Zr_xTi_{1-x})O_3$ ferroelectric FET.[25–27] All these features of resistance show that the ferroelectric-field effect is possibly responsible for the differences in resistance and T_P between P_r^+ and P_r^-. The results also indicate that the ferroelectric polarization induced lattice strain effect dominates over the ferroelectric-field effect in the LCMO/PMN-PT systems.

The effects of converse piezoelectric effect on the resistance of the LCMO films will be discussed in the following sections. First, we positively polarized the PMN-PT substrate in a field of +1.2 kV/mm so that it possesses the converse piezoelectric effect. Figure 5 shows the resistance response of the LCMO film (~25 nm) at 200 K as a function of time while low fields of ±0.12 kV/mm (which corresponds to ~50 V voltage applied to the PMN-PT substrate) were switched on and off. The resistance decreases sharply when a +0.12 kV/mm electric field was switched on and rapidly restores to its initial value upon the removal of the electric field. In contrast, the resistance increases sharply when a negative electric field (−0.12 kV/mm) was switched on and also restores to its initial value upon the removal of the electric field. Moreover, the resistance can be repeatedly modulated between the low- and high-resistance states by switching the electric field between +0.12 and −0.12 kV/mm.

To further examine the resistance change caused by the application of electric fields, we measured the resistance response of the LCMO film at 200 K as a function of time by applying a sinusoidal ac electric field to the positively polarized PMN-PT substrate. The sinusoidal ac electric field with a frequency of 0.1 Hz [Fig. 6(a)] is given by

$$E = 0.12 \sin \theta \ (\text{kV/mm}). \quad (1)$$

As seen in Fig. 6(b), the resistance of the LCMO film was modulated with the same frequency as that of the sinusoidal ac electric field. Note that the resistance in Fig. 6(b) has been normalized to that for $E=0$ kV/mm, i.e., $\Delta R = R(E) - R(0)$, where $R(E)$ and $R(0)$ are the resistance under electric field

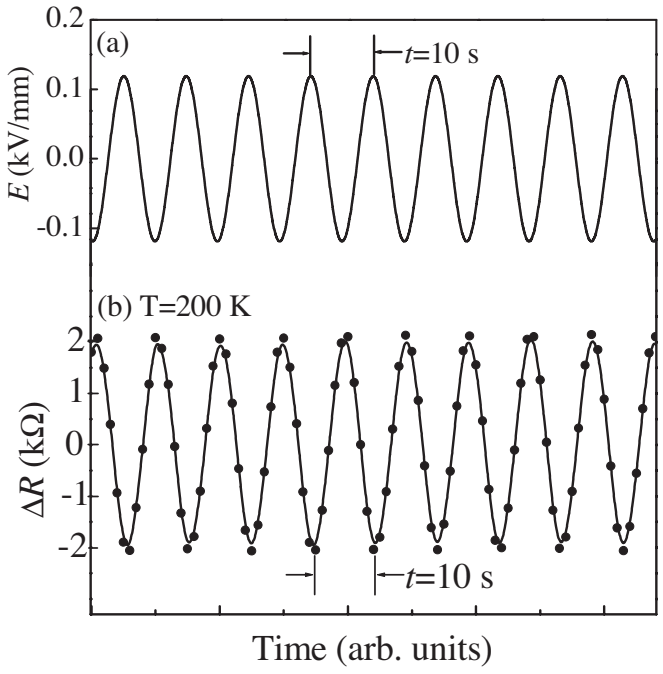

FIG. 6. (a) A 0.12 kV/mm sinusoidal ac electric field with a frequency of 0.1 Hz. (b) Resistance response of the LCMO film as a function of time while the 0.12 kV/mm sinusoidal ac electric field was applied to the positively polarized PMN-PT substrate.

and zero electric field, respectively. ΔR can be described as

$$\Delta R = 2.1 \sin(\theta + \pi)\ (\mathrm{k}\Omega). \tag{2}$$

We note that the phase difference between the sinusoidal electric field and ΔR is π, which implies that the positive maximum in the electric field corresponds to the minimum of the resistance while the negative maximum in the electric field corresponds to the maximum of the resistance. These sinusoidal electric-field-induced changes in the resistance are, in fact, consistent with those induced by dc electric fields. Combining Eq. (1) with Eq. (2), the relation between ΔR and E can be drawn and expressed as

$$\Delta R = -17.5E\ (\mathrm{k}\Omega), \tag{3}$$

where the unit for E is kV/mm. Equation (3) indicates that the change in resistance is linearly dependent on the electric field applied to the PMN-PT substrate. We note that the gate leakage current (I_g) may influence the resistance of the LCMO film.[30] We have measured I_g and found that it was less than 0.2 nA under a 0.12 kV/mm bias field. Such leakage current is negligible as compared with the source/drain current (10 μA). Thus, the modulation of the resistance of the LCMO film upon the application of dc/ac fields cannot be explained in terms of the leakage current. Moreover, it should be pointed out that the PMN-PT substrate had been polarized before the measurements of the resistance of the LCMO film when the PMN-PT substrate was subjected to the 0.12 kV/mm sinusoidal ac electric field. Such a field (i.e., 0.12 kV/mm) is much lower than the coercive field of PMN-PT and thus cannot change the polarization state of the PMN-PT at 200 K. Because of this, one can conclude that

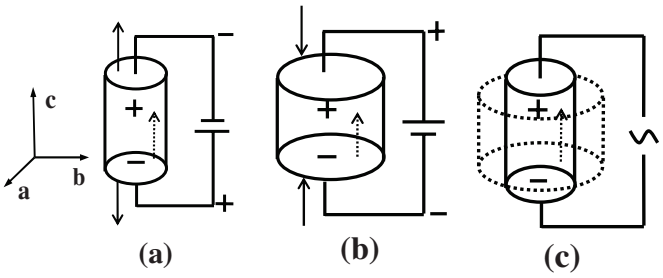

FIG. 7. Schematic diagrams showing the electric-field-induced elongation, compression, and vibration of the lattice of PMN-PT substrate via the converse piezoelectric effect. The dotted arrows represent the direction of the polarization.

the modulation of the resistance of the LCMO film does not result from an injection of charge carriers from the PMN-PT into the LCMO film.

A ferroelectric material exhibits the piezoelectric effect and the converse piezoelectric effect after it has been polarized. This means that electric charges appear on the surfaces of polarized ferroelectric material when a mechanic stress is exerted on it, and conversely a strain is induced in the material when it is subjected to an electric field.[31] Based on the understanding of the converse piezoelectric effect, the modulation of the resistance upon the application of dc/ac electric fields to the PMN-PT substrate can be understood as follows. When a positive electric field is applied to the positively polarized PMN-PT substrate, the lattice of the PMN-PT substrate will expand along the c axis and contract perpendicular to that direction [Fig. 7(a)], imposing in-plane compressive strains on the LCMO film and consequently a decrease in the resistance of the LCMO film. When the electric field is switched off, the lattice of the PMN-PT rapidly restores to its initial positively polarized state. Accordingly, the strain state of the LCMO film restores to its initial value, hence the resistance returns to its initial value. In contrast, upon the application of a negative electric field to the positively polarized PMN-PT substrate, the lattice of the PMN-PT will contract along the c axis and expand perpendicular to that direction [Fig. 7(b)]. Such changes will impose in-plane tensile strains on the LCMO film, causing an increase in the resistance. If an ac electric field is applied to the polarized PMN-PT substrate, the lattice of the PMN-PT will vibrate with the same frequency as that of the driving ac electric field [Fig. 7(c)]. As a result, the strain state and resistance of the LCMO film are modulated with the same frequency as that of the driving ac electric field. Therefore, the modulation of resistance upon the application of dc/ac fields to the PMN-PT substrate can be understood in terms of the induced lattice strain in the LCMO film caused by the converse piezoelectric effect of the PMN-PT.

To further clarify that the modulation of the resistance of the LCMO film is strain-induced, we measured the resistance and strain hysteresis at 300 K as a function of bipolar gate voltages for the LCMO films and the PMN-PT substrates, respectively. Figure 8 shows the resistance hysteresis loops of the LCMO films with thicknesses of ~25 and 75 nm, respectively. It can be seen that both resistance hysteresis loops are of a butterflylike shape. This feature is different

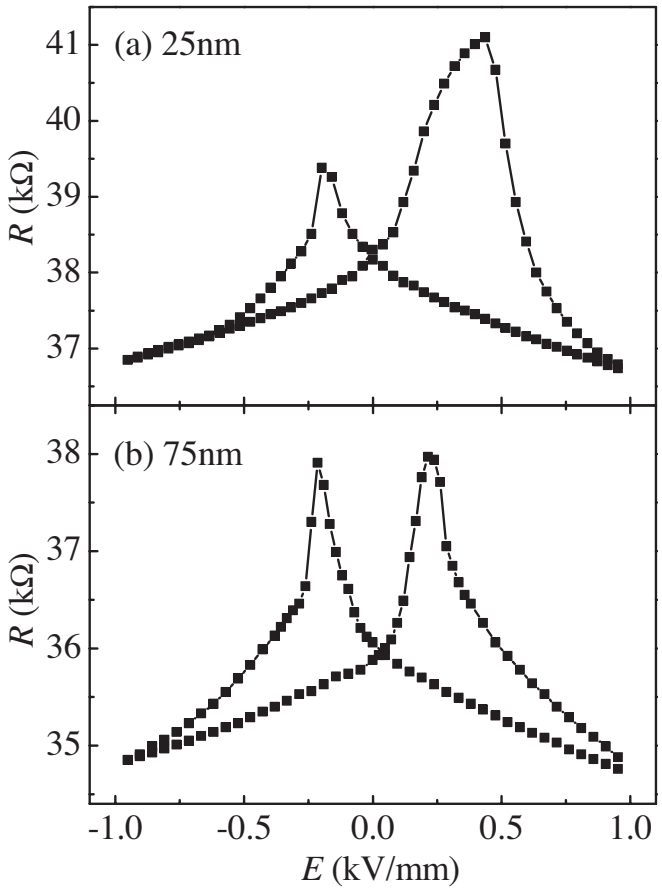

FIG. 8. Resistance hysteresis as a function of gate electric fields at 300 K for LCMO films with thicknesses of ~25 nm (a) and ~75 nm (b), respectively.

from the square resistance hysteresis loops observed in $La_{0.8}Ca_{0.2}MnO_3/Pb(Zr_{0.2}Ti_{0.8})O_3$ (Ref. 24) and $La_{1-x}Ba_xMnO_3/Pb(Zr_xTi_{1-x})O_3$ (Ref. 27) ferroelectric FET, where the ferroelectric-field effect plays a key role in determining the resistance. It is clear that the hysteretic resistance loops agree with the butterflylike strain hysteresis loop stemming from the converse piezoelectric effect of the PMN-PT substrate, as shown in Fig. 9. Thus, one can identify that the modulation of the resistance in the LCMO films is mainly strain-induced. Note that similar modulation of the resistance caused by the converse piezoelectric effect induced lattice strain has also been observed in $La_{0.7}Sr_{0.3}MnO_3/PbZr_{0.52}Ti_{0.48}O_3$ and $La_{0.7}Sr_{0.3}MnO_3/(1-x)Pb(Mg_{1/3}Nb_{2/3})O_3-xPbTiO_3$ ($x\sim0.28$) field effect device.[32,33] Possibly due to the ferroelectric-field effect, the resistance hysteresis loop for the thinner LCMO film (~25 nm) shows an asymmetrical shape while that for the thicker LCMO film (~75 nm) is approximately symmetrical.

To quantify the converse piezoelectric effect induced lattice strain on the resistance in the LCMO film, we measured the resistance (R) in the LCMO film and the lattice strain in the PMN-PT substrate as a function of the electric field E applied to the PMN-PT layer, and the results are shown in Figs. 10 and 11, respectively. The resistance at 77, 200, and 300 K decreases linearly with increasing electric field. The

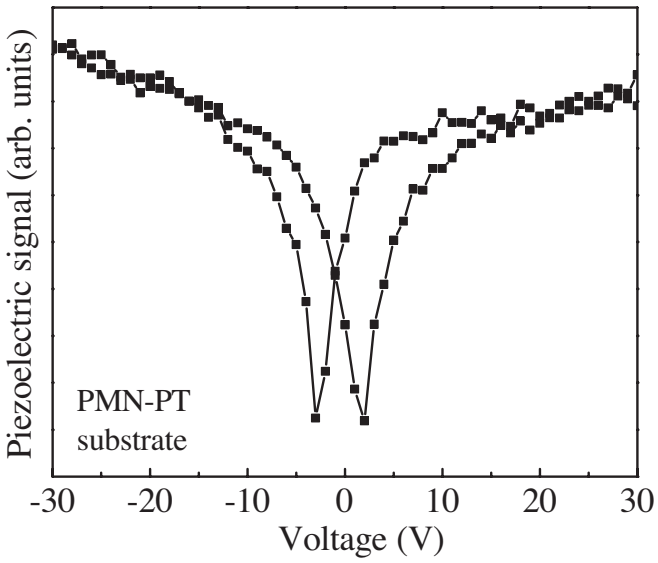

FIG. 9. Electric-voltage dependence of the piezoelectric signal at 300 K for the PMN-PT substrate, which is in proportional to the in-plane strain of the PMN-PT substrate.

relation between R and E at 300 K can be described by

$$R(E) = R(0) - aE, \tag{4}$$

where a is a positive constant. As shown in the inset of Fig. 11, with increasing electric field the PMN-PT(002) reflection shifts to lower 2θ angles being similar to that reported in Ref. 34, indicating that the electric field induces lattice strains in the PMN-PT substrate. The relation between the electric-field induced out-of-plane strain (ε_{zz}) in the PMN-PT substrate and the electric field E can be described by

$$\varepsilon_{zz} = bE(\%), \tag{5}$$

where b is a positive constant. ε_{zz} was estimated using the equation $\varepsilon_{zz}=[c_{zz}(E)-c_{zz}(0)]/c_{zz}(0)$, where $c_{zz}(E)$ and $c_{zz}(0)$ are the lattice parameter c of the PMN-PT under electric field and zero electric field, respectively. Thus, one can obtain a relation between the resistance and the ε_{zz} by combining Eq. (4) with Eq. (5),

$$R(E) = R(0) - a\varepsilon_{zz}/b. \tag{6}$$

Since the converse piezoelectric effect induces an in-plane compressive strain in the PMN-PT substrate when a positive electric field is applied to the positively polarized PMN-PT, and with in-plane strain $\varepsilon_{xx}=\varepsilon_{yy}<0$ (compressive strain) and ν=Poisson's ratio, the relation between ε_{zz} and ε_{xx} can be expressed as[35]

$$\varepsilon_{zz} = -\frac{2\nu}{1-\nu}\varepsilon_{xx}. \tag{7}$$

Combining Eq. (6) with Eq. (7), the relation between the resistance in the LCMO film and the induced in-plane strain in the PMN-PT substrate is given by

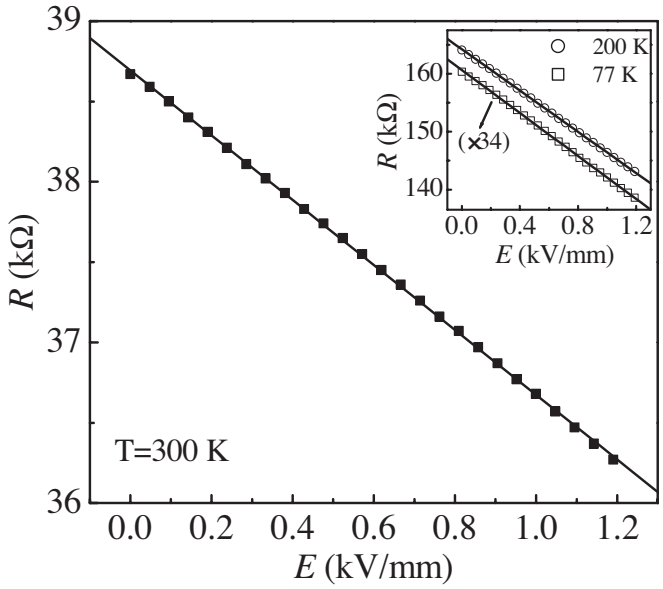

FIG. 10. Resistance of the LCMO film at 300 K as a function of the electric field applied to the positively polarized PMN-PT substrate. The solid line is the fitting using Eq. (4). Inset shows the R vs E curves at 77 and 200 K.

$$R(E) = R(0) + \frac{a}{b}\frac{2\nu}{1-\nu}\varepsilon_{xx}. \tag{8}$$

Since ν is a constant at a fixed temperature, Eq. (8) indicates that the resistance is linearly dependent on the induced in-plane strain in the PMN-PT substrate. This implies that the relative change in resistance ($\Delta R/R$) due to substrate-induced lattice strain is proportional to the relative change in the in-plane strain in the substrate.

IV. CONCLUSION

Thin films of $La_{0.75}Ca_{0.25}MnO_3$ (LCMO) have been grown on ferroelectric PMN-PT single-crystal substrates. The ferroelectric polarization in the PMN-PT substrate imposes in-plane compressive strains on the LCMO films, leading to a decrease in resistance and an upward shift in Curie temperature of the LCMO films. We have found that the strain state and resistance of the LCMO films can be modulated by the converse piezoelectric effect of the PMN-PT, and identified that the ferroelectric polarization and converse piezoelectric effect induced lattice strain effects dominate over the field effect in the LCMO/PMN-PT systems. Moreover, we established a quantitative relation between the resistance in the LCMO films and the induced in-plane strains in the PMN-PT substrates. Since the PMN-PT have excellent electromechanic, optical, ferroelectric, piezoelectric, and converse piezoelectric properties, the combination of these properties with the rich physics in manganites may lead to novel functional devices.

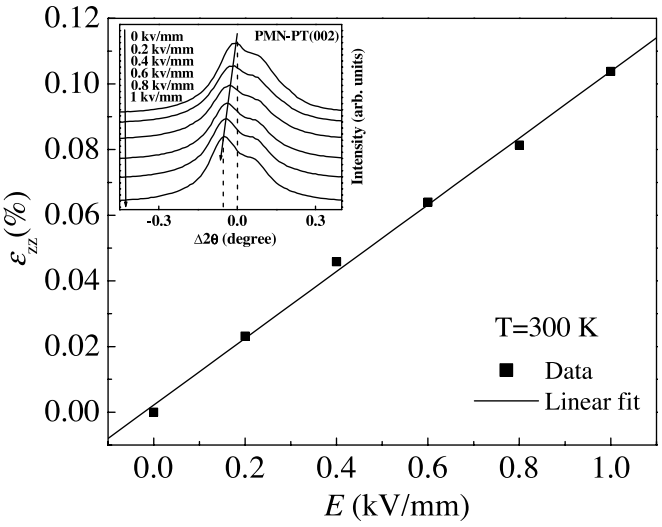

FIG. 11. Out-of-plane strain in the PMN-PT substrate at 300 K as a function of the electric field applied to the positively polarized PMN-PT substrate; the solid line is the fitting using Eq. (5). Inset shows the PMN-PT(002) reflections under different electric fields. 2θ angles have been normalized to that for $E=0$ kV/mm.

ACKNOWLEDGMENTS

This work was supported by the Postdoctoral Fellowship Scheme (Program No. G-YX40) and the Centre for Smart Materials of The Hong Kong Polytechnic University.

*Electronic address: zrk@ustc.edu

[1] *Colossal Magnetoresistive Oxides*, edited by Y. Tokura (Gordon & Breach, Tokyo, 1999).
[2] C. A. Perroni, V. Cataudella, G. De Filippis, G. Iadonisi, V. Marigliano Ramaglia, and F. Ventriglia, Phys. Rev. B **68**, 224424 (2003).
[3] K. H. Ahn and A. J. Millis, Phys. Rev. B **64**, 115103 (2001).
[4] A. J. Millis, T. Darling, and A. Migliori, J. Appl. Phys. **83**, 1588 (1998).
[5] X. J. Chen, S. Soltan, H. Zhang, and H.-U. Habermeier, Phys. Rev. B **65**, 174402 (2002).
[6] X. J. Chen, H.-U. Habermeier, H. Zhang, G. Gu, M. Varela, J. Santamaria, and C. C. Almasan, Phys. Rev. B **72**, 104403 (2005).
[7] Y. Suzuki, H. Y. Hwang, S.-W. Cheong, and R. B. van Dover, Appl. Phys. Lett. **71**, 140 (1997).
[8] M. Ziese, H. C. Semmelhack, and K. H. Han, Phys. Rev. B **68**, 134444 (2003).
[9] R. A. Rao, D. Lavric, T. K. Nath, C. B. Eom, L. Wu, and F. Tsui, J. Appl. Phys. **85**, 4794 (1999).
[10] J. Zhang, H. Tanaka, T. Kanki, J. H. Choi, and T. Kawai, Phys. Rev. B **64**, 184404 (2001).
[11] G. Q. Gong, A. Gupta, G. Xiao, P. Lecoeur, and T. R. McGuire, Phys. Rev. B **54**, R3742 (1996).

[12] T. Kanki, H. Tanaka, and T. Kawai, Solid State Commun. **114**, 267 (2000).
[13] T. Kanki, T. Yanagida, B. Vilquin, H. Tanaka, and T. Kawai, Phys. Rev. B **71**, 012403 (2005).
[14] H. L. Ju, K. M. Krishnan, and D. Lederman, J. Appl. Phys. **83**, 7073 (1998).
[15] A. Miniotas, A. Vailionis, E. B. Svedberg, and U. O. Karlsson, J. Appl. Phys. **89**, 2134 (2001).
[16] T. Kanki, H. Tanaka, and T. Kawai, Phys. Rev. B **64**, 224418 (2001).
[17] P. Murugavel, J. H. Lee, J. G. Yoon, T. W. Noh, J.-S. Chung, M. Heu, and S. Yoon, Appl. Phys. Lett. **82**, 1908 (2003).
[18] O. I. Lebedev, G. Van Tendeloo, S. Amelinckx, B. Leibold, and H.-U. Habermeier, Phys. Rev. B **58**, 8065 (1998).
[19] K. A. Thomas, P. S. I. P. N. de Silva, L. F. Cohen, A. Hossain, M. Rajeswari, T. Venkatesan, R. Hiskes, and J. L. MacManus-Driscoll, J. Appl. Phys. **84**, 3939 (1998).
[20] H. Cao, F. M. Bai, J. F. Li, D. Viehland, G. Y. Xu, H. Hiraka, and G. Shirane, J. Appl. Phys. **97**, 094101 (2005).
[21] R. Zhang, B. Jiang, and W. W. Cao, Appl. Phys. Lett. **82**, 787 (2003).
[22] H. S. Luo, G. S. Xu, H. Q. Xu, P. C. Wang, and Z. W. Yin, Jpn. J. Appl. Phys., Part 1 **39**, 5581 (2000).
[23] S. Mathews, R. Ramesh, and T. Venkatesan, and J. Benedetto, Science **276**, 238 (1997).
[24] T. Zhao, S. B. Ogale, S. R. Shinde, R. Ramesh, R. Droopad, J. Yu, K. Eisenbeiser, and J. Misewich, Appl. Phys. Lett. **84**, 750 (2004).
[25] T. Wu, S. B. Ogale, J. E. Garrison, B. Nagaraj, A. Biswas, Z. Chen, R. L. Greene, R. Ramesh, T. Venkatesan, and A. J. Millis, Phys. Rev. Lett. **86**, 5998 (2001).
[26] X. Hong, A. Posadas, A. Lin, and C. H. Ahn, Phys. Rev. B **68**, 134415 (2003).
[27] T. Kanki, Y. G. Park, H. Tanaka, and T. Kawai, Appl. Phys. Lett. **83**, 4860 (2003).
[28] S. P. Timoshenko and J. N. Goodier, *Theory of Elasticity* (McGraw-Hill, New York, 1987), Chap. 2.
[29] C. H. Ahn, J.-M. Triscone, and J. Mannhart, Nature (London) **424**, 1015 (2003).
[30] I. H. Inoue, Semicond. Sci. Technol. **20**, S112 (2005).
[31] B. Jaffe, W. R. Cook, Jr., and H. Jaffe, *Piezoelectric Ceramics* (Academic Press, New York, 1971).
[32] C. Thiele, K. Dörr, S. Fähler, L. Schultz, D. C. Meyer, A. A. Levin, and P. Paufler, Appl. Phys. Lett. **87**, 262502 (2005).
[33] C. Thiele, K. Dörr, L. Schultz, E. Beyreuther, and W. M. Lin, Appl. Phys. Lett. **87**, 162512 (2005).
[34] A. A. Levin, C. Thiele, P. Paufler, and D. C. Meyer, Appl. Phys. A: Mater. Sci. Process. **84**, 37 (2006).
[35] Y. F. Lu, J. Klein, C. Höfener, B. Wiedenhorst, J. B. Philipp, F. Herbstritt, A. Marx, L. Alff, and R. Gross, Phys. Rev. B **62**, 15806 (2000).